Structural Damage Identification Using Piezoelectric Impedance Sensing with Enhanced Optimization and Enriched Measurements

Yang Zhang^a, Joshua Dupont^a, Ting Wang^a, Kai Zhou^b, Jiong Tang^a

^aDepartment of Mechanical Engineering, University of Connecticut

^bDepartment of Mechanical Engineering-Engineering Mechanics, Michigan Technological

University

ABSTRACT

Fault parameters in a structure can be identified by matching measurements with model predictions in the parametric space. As high frequency measurements are preferred to uncover small-size damage, piezoelectric impedance/admittance active interrogation has shown promising aspects. Nevertheless, the amount of useful measurement information is generally insufficient to pinpoint damage, and the inverse identification is underdetermined. In this research, we develop a combinatorial enhancement to tackle these challenges. A tunable piezoelectric impedance sensing procedure is developed in which an adaptive inductance element is integrated with the piezoelectric transducer, which will lead to enriched measurement data for the same damage. Subsequently, an intelligent multi-objective particle swarm optimization approach is synthesized to inversely identify the damage location and severity. Case studies are conducted to highlight the accuracy of the damage identification.

Keywords: Structural fault identification, piezoelectric transducer, tunable inductor, particle swarm optimization.

INTRODUCTION

Detecting small-size structural damage at an early stage is crucial in preventing catastrophic failure, reducing maintenance costs, and minimizing structural service interruption. One promising technique is to use piezoelectric transducer that works in high-frequency range to yield the impedance/admittance information through active interrogation [1-3]. These methods are based on the two-way electro-mechanical coupling effect of piezoelectric transducer. Specifically, the piezoelectric transducer that is integrated with the structure can excite the host structure by applying frequency-sweeping harmonic voltage; at the same time, the piezoelectric transducer can collect response measurements. As such, the change of the piezoelectric impedance/admittance signature due to damage can be used as the damage indicator. In a typical sensitivity-based inverse analysis, impedance/admittance changes are used as inputs, and a linearized sensitivity matrix relates the measurement change to the change of local structural property in each segment. The change of local structural property forms a so-called damage index vector, the dimension of which is the total number of segments of the structure divided to facilitate damage localization and identification [4-6].

As admittance changes are most noticeable only around structural resonant peaks, the measurement information is generally limited. This is commonly the case in structural health monitoring. Thus, direct inversion using a linearized sensitivity matrix generally results in an under-determined problem which may not be easily solved. To mitigate the limited measurement information issue, we can introduce a tunable inductance element into the measurement circuit. Measuring piezoelectric admittance while tuning the inductance to different values will lead to enriched measurement information even for the same damage location and severity [7-9].

Structural damage identification requires solving both the location and severity of damage. Since direct inversion is subject to the under-determinedness challenge, optimization-based inverse analysis has been investigated [6, 10], the objective of which is to minimize the difference between experimental measurement and model prediction in the damage parametric space. Both deterministic optimization [6] and stochastic optimization [10-12] have been used. These algorithms have achieved good results in some damage identification cases. However, as the complexity of the problem increases, these algorithms based on the single search pattern may fall into local optima and miss the true damage scenario. Subsequently, the particle swarm optimization (PSO) algorithm [13] has been adopted and enhanced to improve the performance on damage identification. PSO is used here due to its inherent advantages, such as its ease of implementation, quick convergence, and robustness. However, the algorithm still has the potential issue of premature convergence, thus leading to limited diversity in solutions obtained. To address these limitations, we intend to improve it

by incorporating search strategies aiming at adaptive coefficient selection and local search. Specifically, we develop a mechanism for the PSO to adapt its search dynamically in response to the environment and explore a wider range of the search space. In this new approach, we control the selection of the best position for each particle in the swarm, using a set of probabilistic decision-making rules. The rewards obtained from executing the rules are used to update the probabilities, and the PSO algorithm updates the particle positions accordingly.

The rest of the paper is organized as follows. In Section 2, the measurement enrichment technique using inductive shunt circuit is outlined, and the optimization model is formulated for damage identification. Section 3 elaborates the enhanced optimization method by combining PSO with adaptive local search. In Section 4, case studies are presented where the proposed algorithm is applied to simulation data. Concluding remarks are given in Section 5.

SYSTEM CONFIGURATION AND MEASUREMENT ENRICHMENT

Modeling of piezoelectric transducer integrated system

A piezoelectric transducer is bonded to the host structure, as shown in Figure 1. The external circuit includes a tunable inductor and a resistor. When harmonic voltage is applied, the piezoelectric transducer can actuate the structure and then the electrical response is measured through the electro-mechanical coupling.

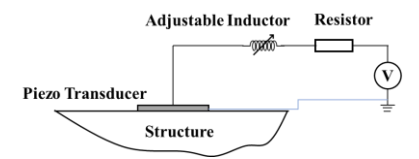


Figure 1. Host structure integrated with piezoelectric transducer and external circuit.

The equations of motion of the host structure integrated with piezoelectric transducer can be derived as [6, 10]

$$\mathbf{M}\ddot{\mathbf{q}} + \mathbf{C}\dot{\mathbf{q}} + \mathbf{K}\mathbf{q} + \mathbf{K}_{1}, Q = \mathbf{0} \tag{1}$$

$$L\ddot{Q} + R\dot{Q} + K_c Q + \mathbf{K}_{12}^T \mathbf{q} = V_{in} \tag{2}$$

where \mathbf{q} is the displacement vector, k_c is the inverse of the capacitance of the piezoelectric transducer; \mathbf{K}_{12} is the electromechanical coupling vector, \mathbf{K} , \mathbf{C} , and \mathbf{M} are the stiffness, damping and mass matrices, respectively, Q is the electrical charge in the piezoelectric circuit, L is inductance, and R is the resistance.. The harmonic voltage excitation can be denoted as $V_{in} = V_0 e^{j\omega t}$. The displacement of structure can be represented as $\mathbf{q} = \mathbf{q}_0 e^{j\omega t}$ and the electrical charge is $Q = Q_0 e^{j\omega t}$. Here V_0 , \mathbf{q}_0 and Q_0 are the respective amplitudes, and ω is the excitation frequency. In this research, we divide the structure into n segments to facilitate damage localization and severity identification. We define damage as percentage change of stiffness in one or multiple segments. The stiffness matrix with damage occurrence, \mathbf{K}_d , can be

expressed as $\mathbf{K}_d = \sum_{i=1}^n \mathbf{K}_h^i \left(1 - \alpha_i\right)$. \mathbf{K}_h^i indicates the stiffness matrix of the *i*th segment under the healthy state.

 $\alpha_i \in [0,1]$ ($i = 1, \dots, n$) is the damage index indicating the stiffness loss of the *i*th segment, which is to be identified. The piezoelectric admittance of the integrated system with structural damage can then be expressed as

$$y_d(\omega) = \frac{\dot{Q}}{V_{in}} = \frac{j\omega}{-\omega^2 L + j\omega R + k_c + \mathbf{K}_{12}^T (\mathbf{K}_d + j\omega \mathbf{C} - \omega^2 \mathbf{M}) \mathbf{K}_{12}}$$
(3)

where *j* is the imaginary unit. Under the assumption of small size damage, we can use Taylor series expansion to express the relation between the damage index and the damage-induced admittance,

$$\Delta y_{m \times 1} = \begin{bmatrix} \Delta Y(\omega_1) \\ \vdots \\ \Delta Y(\omega_m) \end{bmatrix} = \mathbf{S}_{m \times n} \mathbf{\alpha}_{n \times 1}$$
(4)

where **S** is the sensitivity matrix, the vector of admittance change can be obtained at the corresponding excitation frequencies $\boldsymbol{\omega} = \{\omega_1, \omega_2, \ldots, \omega_m\}$, and the damage index vector is written as $\boldsymbol{\alpha} = \{\alpha_1, \alpha_2, \ldots, \alpha_n\}^T$.

It is worth emphasizing that, since the admittance is a function of the inductance, by tuning the inductance in the piezoelectric circuit to a series of values, we can obtain a series of admittance change information for the same damage scenario. This can enrich the measurement information.

2.2 Damage identification formulation

In this section we formulate the optimization objectives for the damage identification problem. As the physics-based damage identification is conducted through the usage of the finite element model where a dense mesh is necessary to guarantee a small wavelength under high frequency working conditions, the number of unknowns in damage identification can be large. While tuning the inductance to different values can enrich the measurement, the inverse identification can still be under-determined. Hereafter, we cast the inverse identification problem into an optimization framework and its model is established as below:

$$\min \|\mathbf{S}\boldsymbol{\alpha} - \Delta y_{\text{meas}}\|_{2} \text{ and } \min \|\boldsymbol{\alpha}\|_{0}$$
 (5)

where Δy_{meas} represents the measurement of change of admittance, and $\|\cdot\|_p$ denotes the l_p norm. Certainly, we need to minimize the difference between the physical measurements and model prediction in damage parametric space. In addition, a true damage scenario in practical situation usually affects only a small number of segments. Here we introduce the sparse regularization by enforcing a sparse constraint. Thus, the second objective function is built to copy with the sparsity of damage index vector. In particular, we select the l_0 norm of α aiming at dealing with the sparsity of index vector. This is a multi-objective optimization that naturally leads to multiple solutions. It is however a challenging problem which requires careful design of algorithmic metaheuristics to achieve a solution set that includes the true damage scenario.

ALGORITHM ENHANCEMENT

3.1 Particle swarm optimization overview

Particle swarm optimization (PSO) is a population based meta-heuristic algorithm that starts with a randomly generated initial population that represents the candidate solutions called particles [13]. During an iteration each particle considers the distance to its personal best position *pbest*, the distance to the global best position *gbest*, and its current velocity and position to update the position, i.e.,

$$v_{i}(t+1) = zv_{i}(t) + c_{1}r_{1}(p_{\text{best}i}(t) - x_{i}(t)) + c_{2}r_{2}(g_{\text{best}}(t) - x_{i}(t))$$
(6a)

$$x_i(t+1) = x_i(t) + v_i(t+1)$$
(6b)

where x(t) represents the position of the *i*th particle in *t*th iteration, v(t) is the velocity of the *i*th particle in the *t*th iteration, w is the inertia weight which reflects the tendency of the particles to maintain their previous speed, and c_1 and c_2 are acceleration coefficients. c_1 regulates how much the particle trusts its own experience, and c_2 represents the trend of particles approaching the best position of the entire swarm. r_1 and r_2 are two random numbers from uniform distribution over the range (0, 1).

3.2 Rationale for improvement

The rationale of improvement comes from Learning Automata which can be considered an abstract decision-making entity situated in a stochastic environment that determines the optimal action through a set of actions and by frequent interactions with the environment [14]. An automaton selects an action from a probability distribution, applies it to the environment, and receives reinforcement. The learning algorithm updates the action probabilities based on the feedback. By repeating this process, the automaton increases the probability of selecting better actions that elicit favorable responses from the environment. It involves the quadruple (α , β , p, T). The linear reward-penalty algorithm (L_{rp}) is one of the various learning algorithms [14]. Here β ranges from 0 to 1. The learning model T for L_{rp} scheme to update the state probability vector p after receiving the reinforcement signal β is given by Equation (7a) when $\beta = 0$ (favorable

response), and Equation (7b) when $\beta = 1$ (unfavorable response). Let α_i be the action chosen at time t as using the distribution p(t).

$$p_{j}(k+1) = \begin{cases} p_{j}(k) + a(1-p_{j}(k)) & \text{if } i = j \\ p_{j}(k)(1-a) & \text{if } i \neq j \end{cases}$$

$$(7a)$$

$$p_{j}(k+1) = \begin{cases} p_{j}(k) + a(1-p_{j}(k)) & \text{if } i = j \\ p_{j}(k)(1-a) & \text{if } i \neq j \end{cases}$$

$$p_{j}(k+1) = \begin{cases} p_{j}(k)(1-b) & \text{if } i = j \\ \frac{b}{r-1} + p_{j}(k)(1-b) & \text{if } i \neq j \end{cases}$$
(7a)

where parameters a and b represent reward and penalty parameters, respectively. Here a=b=0.01.

3.3 An enhanced MOPSO

To help the algorithm jump out of potential local minima, we combine multi-objective particle swarm optimization with the abovementioned rationale. The parameters in PSO algorithm play key role in balancing the exploration and exploitation. The expected goal is to achieve an adaptive coefficient selection. Therefore, we can develop several coefficient variation strategies to form an action repository. Then the adaptation process will be realized. First, Time varying inertia weight proposed in [15] is utilized here, which is conducive to early exploration and later exploitation:

$$\omega^t = \omega_{\text{max}} - (\omega_{\text{max}} - \omega_{\text{min}}) t / t_{\text{max}}$$
 (8)

where t_{max} is the maximum number of iterations, t is the current iteration. ω_{min} and ω_{max} are the initial and final values of the inertia weight. This inertia weight strategy can lead to a fast convergence speed, but it also tends to make the algorithm fall into a local optimum, especially for complex multimodal problems. Thus, time varying acceleration coefficients [16] are used to enhance the global search ability during early stages and the convergence toward the global optima during the later stages. This development is achieved by modifying two acceleration coefficients c_1 , c_2 .

$$c_1^t = c_1^{\max} - \left(c_1^{\max} - c_1^{\min}\right) \frac{t}{t_{\max}} \text{ and } c_2^t = c_2^{\max} + \left(c_2^{\max} - c_2^{\min}\right) \frac{t}{t_{\max}}$$
(9)

where c_1^{\min} , c_2^{\min} are the initial values of c_1 and c_2 , c_1^{\max} and c_2^{\max} are the final values of the c_1 and c_2 , respectively. t is the current iteration number, and t_{max} is the maximum number of allowable iterations.

However, in the optimization process, time varying acceleration coefficients still run risk of inappropriate adjustment between social and cognitive experiences. To tackle this, a mutation strategy is adopted to perform perturbation on the personal best of the particle and provide extra diversity for it to jump out from local optima [17]. Here we refine the strategy by defining a variable *count* to repeat the strategy *count* times. In the mutation strategy, a randomly selected dimension in the personal best of the particle is perturbed using the expression as follows:

$$tempP_{Besti,d} = \begin{cases} P_{Besti,d} + r_d \cdot (vMax_d - vMin_d) & if \text{ rand } > 0.5 \\ P_{Besti,d} - r_d \cdot (vMax_d - vMin_d) & if \text{ rand } \le 0.5 \end{cases}$$
(10)

Here $P_{Besti.d}$ refers to the d-th dimension of personal best of the i-th population, r_d is a random number obtained from the normal distribution. $R_{\text{max}} = 1$ and $R_{\text{min}} = 0.1$, suggested in [17], are the maximum and minimum perturbation ranges, respectively. it is the current number of iterations and maxIter is the maximum iteration of the algorithm. The personal best will be replaced by the temporary personal best if the latter dominates the former and a positive response will be given; otherwise, the personal best remains unchanged. The probability for the corresponding action will be updated accordingly. Similarly, attention is paid to the global best to help the global best take a walk around itself and see if it can jump out of its current position and find a better one. A random perturbation is generated based on the same norm distribution in previous mutation for personal best. At this time, if the temporary global best is dominating the global best, then it will replace the old one. The feedback from the environment will help to update the probability distribution.

$$tempL_{Best,d} = L_{Best,d} + normrnd(\mu, R^2)$$
(11)

CASE STUDY

In this section, we present case studies to demonstrate and verify the performance of the proposed damage identification framework using piezoelectric admittance. The host structure is a plate, as shown in Figure 2. The piezoelectric transducer is attached to the plate at the intersection of the center lines. The dimensions for the host plate and the piezoelectric transducer are labelled in the figure. The thickness of the piezoelectric transducer is 3.5 mm, and that of the plate is 3.875 mm. The plate is made of aluminum with Young's modulus 73 GPa, density 2769.84 kg/m³. The piezoelectric transducer is the type SM411 from Steiner & Martins, Inc. The material constants of the piezoelectric transducer are $E_{11} = 74$ GPa, $E_{33} = 54$ GPa, $E_{31} = -10.4$ (10^{-3} Vm/N), $E_{33} = 24.2$ (10^{-3} Vm/N) and $E_{31} = -210$ (10^{-12} m/V). The sweeping frequency is from 3,870 Hz to 4,200 Hz with 200 frequency points. To enrich the measurements, here the adjustable inductor is tuned to 0.181, 0.185 and 0.189 H, respectively. The admittance curves obtained are plotted in Figure 3. All analyses are implemented using an in-house MATLAB code. Based on the finite element model, we can obtain the corresponding sensitivity matrices as shown in Equation (4).

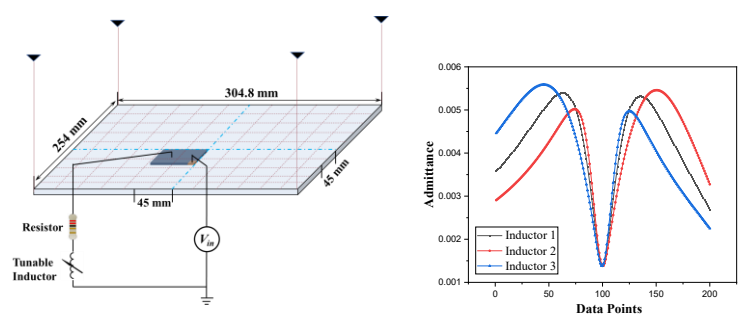


Figure 2. Schematic of structure to be monitored (left), and admittance curves with different inductors (right).

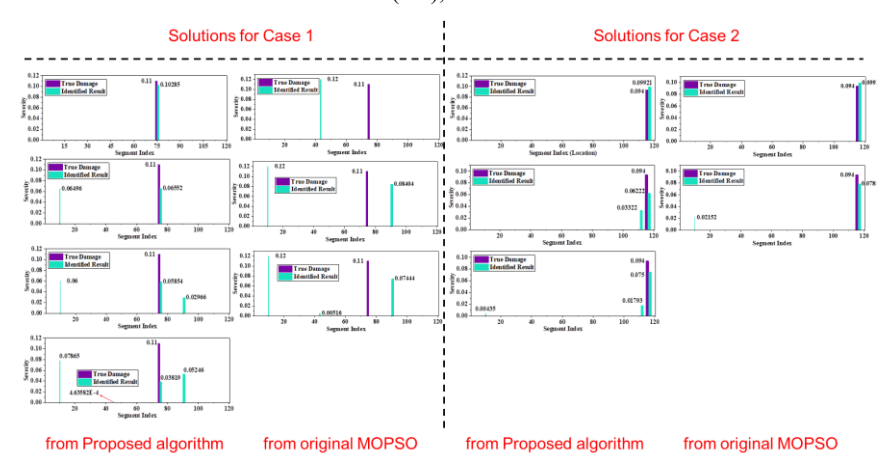


Figure 3. Identified results for Case 1 and Case 2.

The plate structure is divided into 120 segments, each of which is susceptible to damage occurrence. Two cases are analyzed. In the first scenario, the damage is assumed to be located at the 75th segment with 11.0% equivalent stiffness reduction. In the second scenario, the damage is located at the 116th segment with a smaller damage severity of 9.4%. By solving the optimization model using the enhanced algorithm, the identified results are plotted in Figure 3. The results of Case 1 indicate that the proposed algorithm produces four solutions, all of which accurately identify the true damage location. In contrast, although the original MOPSO leads to three solutions, none of them identifies the true damage scenario. This demonstrates the accuracy of the proposed algorithm in damage identification. The results of Case 2 show that both the proposed algorithm and the original MOPSO can identify the true damage location. However, in terms of solution diversity, the proposed algorithm outperforms the original MOPSO.

In this research, we introduce tunable inductor to enrich the measurements. The hypothesis is that with more information for the same damage condition, the identification result will be more accurate, and the number of solutions obtained will gradually decrease. To examine this point, we use different numbers of inductance tuning, and observe the number of

solutions, as shown in Figure 4. The horizontal axis indicates the number of inductance tunings used in the monitoring process, and the vertical axis indicates the average number of solutions obtained. S represents a single measurement. It can be observed that as the number of tunings used increases, the number of obtained solutions decreases. In addition, when only one inductance is used to obtain admittance information as input, the accuracy of the solutions obtained is 0, indicating that no solution can identify the true damage location. When admittance information obtained from two inductors is used as input, the accuracy begins to increase. With the increase of the number of tunings, accuracy shows an increasing trend.

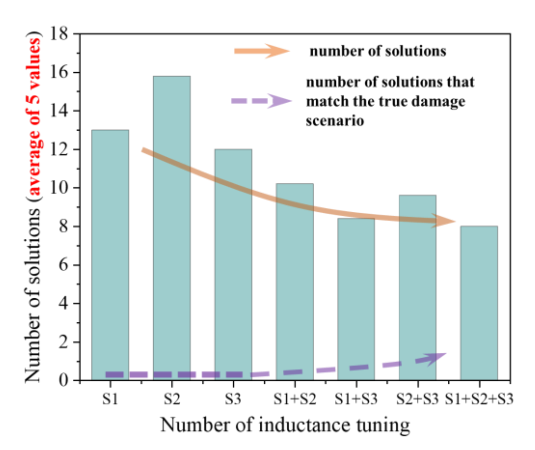


Figure 4. Number of solutions with different number of measurements used, (S1: inductance = 0.181 H, S2: inductance = 0.185 H, S3: inductance = 0.189 H).

CONCLUSION

In this research, we explore the advancement of piezoelectric admittance based active interrogation by enriching the measurement and enhancing the inverse identification. A tunable inductor is introduced into the measurement circuit. This can not only provide an additional peak around resonant frequency, but also generate a series of admittance curves by adjusting the value of the inductor. Moreover, we aim to improve the inverse analysis by incorporating strategies that adaptively select coefficients to improve local search into multi-objective particle swarm optimization. Two case studies demonstrate performance enhancement.

ACKNOWLEDGMENT

This research is supported in part by This research is supported in part by a Space Technology Research Institutes grant (number 80NSSC19K1076) from NASA's Space Technology Research Grants Program and in part by the National Science Foundation under grant CMMI-1825324.

REFERENCES

- [1] Park, G., Sohn, H., Farrar, C.R. and Inman, D.J., Overview of piezoelectric impedance-based health monitoring and path forward. Shock and vibration digest, 35(6), pp.451-464 (2003).
- [2] Fan, X. and Li, J., Damage Identification in Plate Structures Using Sparse Regularization Based Electromechanical Impedance Technique. Sensors, 20(24), p.7069 (2020).
- [3] Zhang, Y., Zhou, K. and Tang, J., 2022, April. Structural damage identification using inverse analysis through optimization with sparsity. In Sensors and Smart Structures Technologies for Civil, Mechanical, and Aerospace Systems 2022 (Vol. 12046, pp. 36-40). SPIE.
- [4] Zhou, K., Zhang, Y. and Tang, J. Order-Reduced Modeling-Based Multi-Level Damage Identification Using Piezoelectric Impedance Measurement. IFAC-PapersOnLine, 55(27), pp.341-346 (2022).
- [5] Shuai, Q., Zhou, K., Zhou, S. and Tang, J., Fault identification using piezoelectric impedance measurement and model-based intelligent inference with pre-screening. Smart Materials and Structures, 26(4), p.045007 (2017).
- [6] Cao, Pei, Shuai Qi, and Jiong Tang, Structural damage identification using piezoelectric impedance measurement with sparse inverse analysis. Smart Materials and Structures, 27(3): 035020 (2018).

- [7] Kim, J., Harne, R.L. and Wang, K.W. Enhancing structural damage identification robustness to noise and damping with integrated bistable and adaptive piezoelectric circuitry. Journal of Vibration and Acoustics, 137(1) (2015).
- [8] Kim, J. and Wang, K.W. Electromechanical impedance-based damage identification enhancement using bistable and adaptive piezoelectric circuitry. Structural Health Monitoring, 18(4), pp.1268-1281 (2019).
- [9] Zhang, X., Wang, H., Hou, B., Xu, J. and Yan, R. 1D-CNN-based damage identification method based on piezoelectric impedance using adjustable inductive shunt circuitry for data enrichment. Structural Health Monitoring, 21(5), pp.1992-2009 (2022).
- [10] Cao, P., Zhang, Y., Zhou, K. and Tang, J. A reinforcement learning hyper-heuristic in multi-objective optimization with application to structural damage identification. Structural and Multidisciplinary Optimization, 66(1), p.16 (2023).
- [11] Ding, Z., Li, J. and Hao, H., Structural damage identification using improved Jaya algorithm based on sparse regularization and Bayesian inference. Mechanical Systems and Signal Processing, 132, pp.211-231(2019).
- [12] Minh, H.L., Khatir, S., Wahab, M.A. and Cuong-Le, T., An Enhancing Particle Swarm Optimization Algorithm (EHVPSO) for damage identification in 3D transmission tower. Engineering Structures, 242, p.112412 (2021).
- [13] Coello, C.A.C., Pulido, G.T. and Lechuga, M.S., Handling multiple objectives with particle swarm optimization. IEEE Transactions on evolutionary computation, 8(3), pp.256-279 (2004).
- [14] Rezvanian, A., Moradabadi, B., Ghavipour, M., Daliri Khomami, M.M., Meybodi, M.R., Rezvanian, A., Moradabadi, B., Ghavipour, M., Daliri Khomami, M.M. and Meybodi, M.R. Introduction to learning automata models. Learning Automata Approach for Social Networks, pp.1-49 (2019).
- [15] Shi, Y. and Eberhart, R.C. Empirical study of particle swarm optimization. In Proceedings of the 1999 congress on evolutionary computation-CEC99 (Cat. No. 99TH8406) (Vol. 3, pp. 1945-1950). IEEE (1999).
- [16] Ratnaweera, A., Halgamuge, S.K. and Watson, H.C. Self-organizing hierarchical particle swarm optimizer with time-varying acceleration coefficients. IEEE Transactions on evolutionary computation, 8(3), pp.240-255 (2004).
- [17] Lim, W.H. and Isa, N.A.M. Two-layer particle swarm optimization with intelligent division of labor. Engineering Applications of Artificial Intelligence, 26(10), pp.2327-2348 (2013).